

Fusion–fission dynamics in the superheavy nucleus production

G GIARDINA¹, P D'AGOSTINO¹, G FAZIO¹, M HERMAN², A I MUNINOV³,
A NASIROV^{3,4}, G OLIVA¹, R PALAMARA⁵ and R RUGGERI¹

¹Istituto Nazionale di Fisica Nucleare, Sezione di Catania, Dipartimento di Fisica dell'Università di Messina, 98166 Messina, Italy

²IAEA, A-1400 Vienna, Austria

³Institute of Nuclear Physics, 702132 Ulugbek, Tashkent, Uzbekistan

⁴Bogoliubov Laboratory of Theoretical Physics, JINR, 141980 Dubna, Russia

⁵Dipartimento PAU dell'Università di Reggio Calabria, 89100 Reggio Calabria, Italy

Abstract. The fusion–fission reaction mechanism leading to the massive nucleus formation is studied. We investigate the superheavy nucleus formation in heavy-ion induced reactions by analysing the evaporation residue (ER) production in order to study the fusion dynamics and the decay properties of nuclei close to the stability island at $Z = 114$. We consider the $^{64}\text{Ni} + ^{208}\text{Pb}$, $^{48}\text{Ca} + ^{238}\text{U}$ and $^{48}\text{Ca} + ^{244}\text{Pu}$ reactions that lead to the $Z = 110$, 112 and 114 superheavy elements respectively.

By using the dinuclear system (DNS) concept of the two interacting nuclei we calculate the quasifission–fusion competition in the entrance channel and the fission–evaporation competition along the de-excitation cascade of the compound nucleus. The dynamics of the entrance channel allows us to determine the beam energy window which is favorable to the fusion, while the dynamic evolution of the compound nucleus on the shell correction to the fission barrier and the dissipative effects influence the fission–evaporation competition in order to obtain the residue nuclei from the superheavy nucleus formation. We also calculate the $\Gamma_n/\Gamma_{\text{tot}}$ ratio at each step of the de-excitation cascade of the compound nucleus and we present a systematics of $\Gamma_n/\Gamma_{\text{tot}}$ (at first step of the cascade) for many reactions that lead to nuclei with $Z = 102$ –114.

Keywords. Quasifission; fusion; fission; evaporation residues; superheavy elements.

PACS Nos 25.70.-z; 25.70.Jj; 27.90.+b

1. Introduction

The synthesis of superheavy nuclei is an interesting and present research field [1–6] but the cross section for the formation of heavy elements by fusion reaction (using Pb, U and Pu targets) decreases down to a very low value that the evaporation residue (ER) production is about few pb or lower. According to the dinuclear system (DNS)-concept the fusion of nuclei is considered as a two stage process: the first stage is the capture (the formation of the DNS after dissipation of some part of the relative kinetic energy and orbital angular momentum); the second stage is the fusion (the transformation of the dinuclear system in the compound nucleus by a continuous multinucleon transfer from a light nucleus to

a heavy one retaining the individuality of nuclei having a shell structure). In this second stage, fusion is in competition with quasifission which is the decay of the dinuclear system in two fragments before the formation of the compound nucleus. Thus, fusion is treated as a motion in the charge (mass) asymmetry variable, and capture and quasifission are a consequence of the relative motion of nuclei in DNS. The energy window for the capture was revealed. If there is no capture, nuclei cannot be fused due to the smallness of the interaction time and the excitation energy generated from the relative kinetic energy. Therefore, the used model [7] is required to analyse the fusion of light nuclei at high energies and the fusion of massive nuclei at all collision energies where quasifission plays a decisive role in decreasing the fusion cross section [8,9]. As a result of the calculation we find that: (i) a number of partial waves with angular momentum lead to capture (i.e., those partial waves which have been trapped in a potential minimum of the entrance channel; the critical value of angular momentum l_{cr} for a given collision energy can be calculated dynamically); (ii) an amount of the excitation energy is available before the complete fusion at given collision energy and impact parameter or orbital angular momentum; (iii) a beam energy window is favorable to the fusion: the low limit (E_{min}) of this window is defined by the dynamical barrier in the entrance channel before the capture. The upper limit (E_{max}) appears because friction forces cannot provide an intense loss of the initial kinetic energy in order to trap the dinuclear system into a pocket.

After fusion, the de-excitation cascade of the compound nucleus was analysed in detail in the framework of the advanced statistical model (ASM) approximation [10]. With this model it is possible to trace the Γ_n/Γ_{tot} values at each step of the de-excitation cascade and to have information on the consequences for the fission process dynamics. The model allows us to consider the influence of the nuclear viscosity and the dynamical dependence of the shell correction to the fission barrier on the calculated ER cross sections.

2. General remarks on the formalism

We study the precompound nucleus dynamics through the evolution of DNS (after capture) to complete fusion (that is in competition with the quasifission process). The excited compound nucleus can undergo fission or emit particles before detecting the reaction products (evaporation residues, or fission fragments, or light particles).

In the suggested model [7], the relevant variables are energies and occupation numbers of single-particle states of nucleons in nuclei (the intrinsic degrees of freedom) and relative motion of nuclei at the first-capture stage, and the mass (charge) asymmetry degrees of freedom at the second stage of fusion. The competition between complete fusion and quasifission of the dinuclear system formed after capture as its further evolution is taken into account by the statistical theory of level densities on the intrinsic fusion barrier which is on the charge asymmetry axis and quasifission barrier which is on the relative distance axis as in [11]. In contrast to [11], the capture probability $T_l^{capture}(E, l)$ is estimated in a dynamic approach, considering the evolution of the coupling between the relative motion of nuclei and intrinsic motion of their nucleons. In the capture stage the system is trapped in a potential wall due to the dissipation of the initial kinetic energy. The formed DNS lives long enough (several 10^{-21} s) to evolve from the projectile-and target-like configuration to become mononucleus (compound nucleus). This evolution corresponds to the motion on the mass (charge) asymmetry axis.

The evaporation residue cross section is related to the partial fusion cross section $\sigma_l^{\text{fus}}(E, l)$, as well as to the probability $W_{\text{sur}}(E, l)$ that the compound nucleus survives fission during the de-excitation cascade at the bombarding energy E :

$$\sigma_{\text{er}}(E) = \sum_{l=0}^{\infty} \sigma_l^{\text{cap}}(E) P_{CN}(E, l) W_{\text{sur}}(E, l), \quad (1)$$

where the partial fusion cross section is $\sigma_l^{\text{fus}} = \sigma_l^{\text{cap}}(E) P_{CN}(E, l)$ and the partial capture cross section is $\sigma_l^{\text{cap}}(E) = \lambda^2 / 4\pi(2l + 1) T_l^{\text{capture}}(E, l)$. The factor $P_{CN}(E, l)$ is used to take into account the decrease of the fusion probability due to dinuclear system break-up competing with fusion. At first this factor was determined in [11].

The calculation of competition between fusion and quasifission processes can be made according to principles of the statistical theory by comparing the level density at the top point (after which the dinuclear system goes to the fusion through smaller mass asymmetry values) of the $U(Z, A; l, R_m)$ driving potential (see figure 1) with the level density at the bottom of the exit barrier pocket in the $V(Z, A; l, \mathbf{R})$ internuclear potential (see figure 2). The driving potential, playing the main role in fusion dynamics, was calculated as follows:

$$U(Z, A; l, R_m) = B_1(Z; A) + B_2(Z_P + Z_T - Z; A_P + A_T - A) + V(Z, A; l, R_m) - B_0, \quad (2)$$

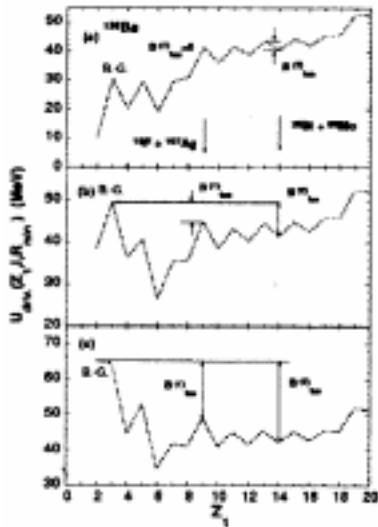


Figure 1. The driving potential (dashed curves) of compound nucleus ^{126}Ba calculated for different values of angular momentum: $l = 0$ (a), $l = 20\hbar$ (b), and $l = 30\hbar$ (c). The different values of the entrance mass asymmetry are shown by arrows ($Z_1 = 9$ and 14). $B_{\text{fus}}^{(1)}$ and $B_{\text{fus}}^{(2)}$ are intrinsic barriers in the way to fusion for the $^{19}\text{F} + ^{107}\text{Ag}$ and $^{28}\text{Si} + ^{98}\text{Mo}$ reactions, respectively.

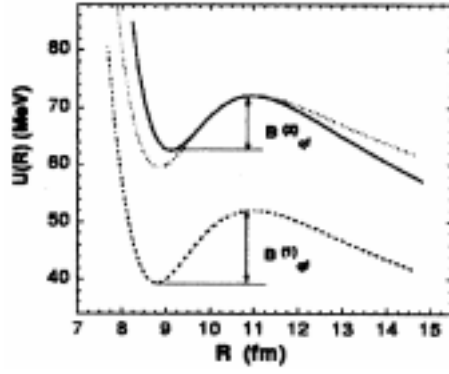


Figure 2. The nucleus–nucleus potential $U(R)$ calculated for the $^{28}\text{Si} + ^{98}\text{Mo}$ (solid curve) and $^{19}\text{F} + ^{107}\text{Ag}$ (dashed curve) reactions as a function of internuclear distance. For an easier comparison of two pockets (in width and depth) the dashed curve is shifted (dotted curve) up to overlapping with the solid curve. $B_{\text{qf}}^{(1)}$ and $B_{\text{qf}}^{(2)}$ are quasifission barriers for the corresponding reactions.

where B_1 and B_2 are the binding energies of the nuclei in a dinuclear system, $V(R_m) = V(Z, A, R_m)$ is the minimum value of the nucleus–nucleus interaction potential at the bottom of the pocket; B_0 is the binding energy of the compound nucleus. For the given total charge and mass numbers, $Z_{\text{tot}} = Z_1 + Z_2$ and $A_{\text{tot}} = A_1 + A_2$, the A/Z ratio of the considered fragment was determined from the minimum value of $U(Z, A; l, R_m)$.

The $T_l^{\text{capture}}(E, l)$ factor is connected with the relative kinetic energy and angular momentum losses which were determined from the equations of motion

$$\mu(\mathbf{R}(t))\ddot{\mathbf{R}} + \gamma_R[\mathbf{R}(t)]\dot{\mathbf{R}}(t) = -\frac{\partial V[\mathbf{R}(t)]}{\partial \mathbf{R}}, \quad (3)$$

$$\frac{dL}{dt} = \gamma_\theta[\mathbf{R}(t)] \left(\dot{\theta} R_{\text{eff}}^2 - \dot{\theta}_1 R_{1\text{eff}}^2 - \dot{\theta}_2 R_{2\text{eff}}^2 \right), \quad (4)$$

where $\mathbf{R}(t)$ is the relative motion coordinate, $\dot{\mathbf{R}}(t)$ is the corresponding velocity; $\dot{\theta}$, $\dot{\theta}_1$ and $\dot{\theta}_2$ are angular velocities of the dinuclear system and its two fragments, respectively, while R_1 and R_2 are the fragment radii. The γ_R and γ_θ friction coefficients, a change of the nucleus–nucleus potential during interaction of nuclei, $V[\mathbf{R}(t)] = V_0[\mathbf{R}(t)] + \delta\hat{V}(\mathbf{R})$, and the dynamic contribution $\delta\mu(\mathbf{R})$ to the reduced mass $\mu(\mathbf{R}) = m_{A_T A_P} / (A_T + A_P) + \delta\mu(\mathbf{R})$ are calculated from the estimation of the coupling term between the relative motion of nuclei and intrinsic excitation of nucleons in them [12].

The dynamics of the capture is sensitive to the nucleus–nucleus potential

$$V_0(\mathbf{R}) = V_C(\mathbf{R}) + V_{\text{nuc}}(\mathbf{R}) + V_{\text{rot}}(\mathbf{R}), \quad (5)$$

where $V_C(\mathbf{R})$, $V_{\text{nuc}}(\mathbf{R})$, and $V_{\text{rot}}(\mathbf{R})$ are the Coulomb, nuclear and rotational potentials, respectively. The nuclear shape is important to calculate the Coulomb and nuclear interaction between colliding nuclei.

By our AMS it was possible to take into account the dynamical aspect of the compound nucleus evolution on the fission–evaporation competition along the de-excitation cascade.

As far as the fission barriers are concerned, we use the rotating droplet model predictions (angular momentum dependent) as parameterized by Sierk [13] and allow for angular momentum and temperature fade-out of the shell corrections [14]. It is expressed by the formula for the actual fission barrier used in our calculations:

$$B_f(J, T) = cB_f^m(J) - f(T)g(J)\delta W, \quad (6)$$

with

$$f(T) = \begin{cases} 1 & T \leq 1.65 \text{ MeV} \\ k \exp(-mT) & T > 1.65 \text{ MeV} \end{cases}$$

and

$$g(J) = \left\{ 1 + \exp[(J - J_{1/2})/\Delta J] \right\}^{-1},$$

where $B_f^m(J)$ is the parameterized macroscopic fission barrier [13] depending on J angular momentum, $\delta W = \delta W_{\text{sad}} - \delta W_{\text{gs}} \simeq -\delta W_{\text{gs}}$ is the microscopic (shell) correction to the fission barrier taken from the tables [15] and the constants for the macroscopic fission barrier scaling, temperature and angular momentum dependencies of the microscopic correction are chosen to be as follows: $c = 1.0$, $k = 5.809$, $m = 1.066 \text{ MeV}^{-1}$, $J_{1/2} = 24\hbar$ (for nuclei with an A mass number of about 210) and $\Delta J = 3\hbar$. These constants were obtained as the result of analysis of a large set of the data on the fissility of nuclei in the Lu–At range obtained in the reactions induced by light (p , t and α) and heavy (^{12}C and ^{18}O) projectiles [14]. This makes our shell corrections become dynamical quantities too. The $J_{1/2}$ parameter slowly decreases increasing the A mass number. For nuclei with $A > 250$ we use $J_{1/2} = 20\hbar$.

The systematics obtained by Bhattacharya *et al* [16] gives the possibility of taking into account the incident energy per nucleon ϵ and compound nucleus mass A_{cn} dependencies of the reduced dissipation coefficient β (the ratio between the γ friction coefficient describing the coupling to the fission degree of freedom and the m reduced mass of the system).

We use the same set of parameters for all superheavy nuclei and there are no free parameters in our calculations. By this model it is possible to trace the $\Gamma_n/\Gamma_{\text{tot}}$ values at each step of the de-excitation cascade.

3. Results and discussion

We present the results of the investigation on massive systems that lead to the formation of the $Z = 110, 112$ and 114 superheavy elements, and we compare our calculation with the available experimental data.

Figure 3 shows the fusion cross section (full line) for the $^{64}\text{Ni} + ^{208}\text{Pb}$ reaction that forms the $^{272}110$ excited compound nucleus by a *cold fusion reaction*. In the same figure we report the quasifission contribution (dotted-dashed line), the evaporation residue cross-section (dashed line) after 1 neutron emission from the excited compound nucleus, and the fission barrier (dotted line). In this figure we also report the experimental data of the

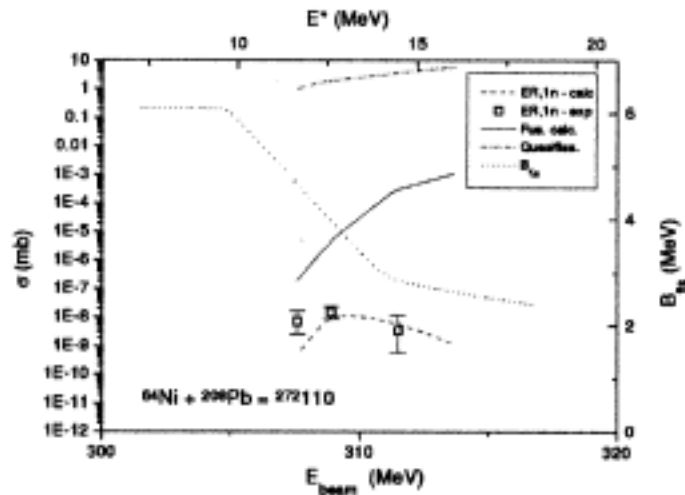


Figure 3. Fusion cross section for reaction $^{64}\text{Ni} + ^{208}\text{Pb} \Rightarrow ^{272}110$.

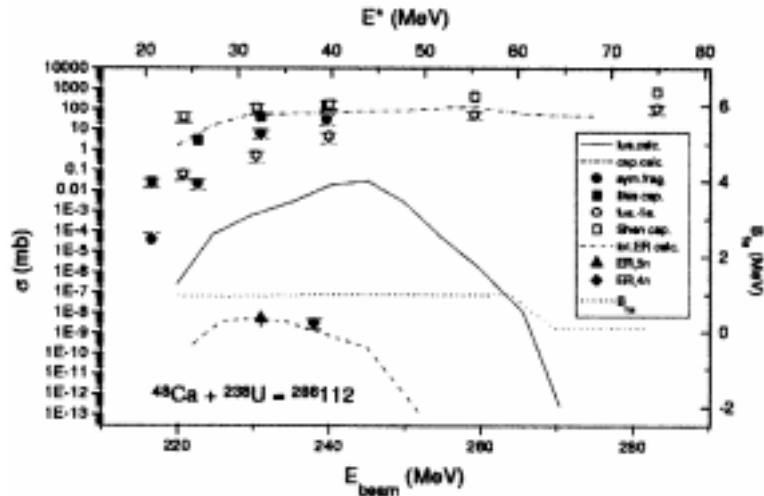


Figure 4. Fusion cross section for reaction $^{48}\text{Ca} + ^{238}\text{U} \Rightarrow ^{286}112$.

evaporation residues [1]. We can observe the full agreement between experimental data and calculation. It is possible to analyse the ratio (10^{-7} – 2×10^{-4}) between the complete fusion and quasifission, and the ratio (2×10^{-3} – 10^{-5}) between the evaporation residue production and fusion. At low beam energies (lower than 307 MeV) the ER cross section is limited by the low value of the fusion formation. At high beam energies (higher than 313 MeV) the ER production decreases because the fission process strongly increases. This last effect is related to the fade-out of the fission barrier, due to the damping of the shell correction.

Figure 4 shows the results obtained for the $^{48}\text{Ca} + ^{238}\text{U}$ reaction that lead to the $^{286}112$ excited compound nucleus. From this figure one can observe the beam energy window

($E_{\text{beam}} \simeq 218\text{--}262$ MeV, corresponding to about $E^* = 21\text{--}58$ MeV) that allows for the complete fusion formation (> 1 nb). In this energy interval and for the above-mentioned *hot fusion reaction*, the ratio between fusion and quasifission is about $10^{-8}\text{--}2 \times 10^{-4}$ and the ratio between the ER cross section and complete fusion is about $10^{-4}\text{--}5 \times 10^{-8}$. At lower beam energies the ER production is limited by the fusion formation, at higher beam energies the ER cross section is limited by both the low fusion formation and the fade-out of the fission barrier ($B_{\text{fis}} < 0.12$ MeV) that strongly increases the fission process.

In figure 5 we report the excitation functions for the $^{48}\text{Ca}(^{238}\text{U}, xn)^{286-xn}112$ reaction after the x ($x = 2, 3, 4$) neutron emission from the excited compound nucleus. In this figure we also report the experimental ER cross section [17] obtained by the $^{286-3n}112$ (triangle) spontaneous fission events. For the $^{286-4n}112$ residual nucleus (diamond) the experimental estimation of the upper limit is reported. The agreement between the calculation and experimental data is very good, even if until now only partial experimental measurements are known. Dotted line is the fission barrier for the compound nucleus (see figures 4 and 5).

In figure 4 the experimental data of capture cross section [17] (full squares) and [18] (open squares), the symmetric fragment cross section [17] (full circles), the ER production [17] after $3n$ (triangle) and $4n$ (diamond) emission and the fusion–fission production [18] (open circles) for the reaction induced by ^{48}Ca (where an intrinsic fusion barrier $B_f \simeq 13.5$ MeV exists) are also reported. In the same figure we report, for comparison, our capture cross section calculation (dashed-dotted line), fusion cross section (full line) and the total ER production (dashed line) after 2, 3 and 4 neutron emission from the excited $^{286}112$ compound nucleus. As one can see, the capture cross section calculation and the total ER calculation are in agreement with the experimental data of [17,18], whereas the fusion cross section calculation is lower than the symmetric fragment production [17] and the fusion cross section [18] extracted from the experimental fragment production. Therefore, the fragment production should be mainly contributed from the quasifission process, whereas the fission products after fusion at the various beam energies can reach the fusion cross section value. In fact, for the beam energy range corresponding to the experimental data of

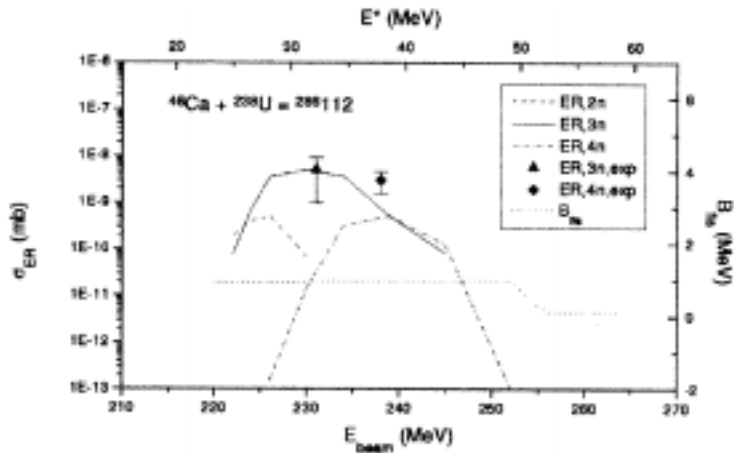


Figure 5. Excitation functions for the $^{48}\text{Ca}(^{238}\text{U}, xn)^{286-xn}112$ reactions.

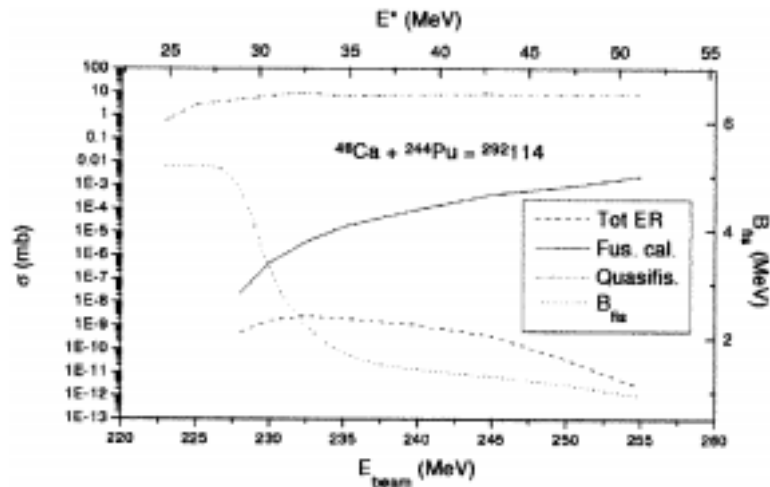


Figure 6. Calculated cross sections for the reaction $^{48}\text{Ca} + ^{244}\text{Pu}$.

ER, the ratio between our ER calculation and the fusion cross section calculation is about 10^{-5} – 10^{-6} , whereas the ratio between the experimental ER production and the experimental symmetric fragment production is about 5×10^{-8} – 5×10^{-9} (corresponding to a very small ER value, considering that the B_{fis} fission barrier is about 1 MeV).

From these considerations it is possible to affirm that by *cold fusion reactions* it is very difficult to synthesize superheavy elements (and to observe the evaporation residue products) because the E_{DNS}^* excitation energy of the dinuclear system (after capture) is generally lower than (or close to) the B_f intrinsic fusion barrier, whereas by *hot fusion reactions* the E_{DNS}^* energy is higher than B_f .

In figure 6 we report the calculation for the $^{48}\text{Ca} + ^{244}\text{Pu}$ reaction that lead to the $^{292}114$ compound nucleus at beam energies of 228–255 MeV, corresponding to excitation energies lower than 52 MeV and the $^{287-290}114$ residue nucleus production. Full line represents the fusion cross section, dashed-dotted line is the quasifission contribution, dashed line is the total ER production after x neutron emission. Dotted line represents the fission barrier against the excitation energy of the compound nucleus. In figure 7 we report the excitation functions for the $^{48}\text{Ca} (^{244}\text{Pu}, xn) ^{292-xn}114$ reaction after the x ($x = 2, 3, 4$ and 5) neutron emission from the compound nucleus. The ER to fusion ratio is included in the 10^{-2} – 10^{-8} range while the fusion to quasifission ratio changes between 10^{-4} – 10^{-7} in the considered energy range.

In figure 8 we present the systematics of the $\Gamma_n/\Gamma_{\text{tot}}$ ratio, at first step of the de-excitation cascade of the compound nucleus, for reactions that lead to heavy and superheavy nuclei with $Z = 102$ – 114 . This figure shows the trend of the $\Gamma_n/\Gamma_{\text{tot}}$ ratio against E^*/B_{fis} for many reactions at different energies. As one can see the $\Gamma_n/\Gamma_{\text{tot}}$ ratio is strongly correlated (within a factor 2) to the E^*/B_{fis} ratio. It is to be noted that the emission of the gamma rays, neutrons, protons and alpha particles is not considered in the present model. This effect (that will be the subject of a future work) can be relevant at higher energies, and can significantly change the $\Gamma_n/\Gamma_{\text{tot}}$ trend at higher E^*/B_{fis} values. Therefore, the trend of the ER production versus the excitation energy (in comparison with the effective fission barrier) has the same behaviour for all investigated reactions.

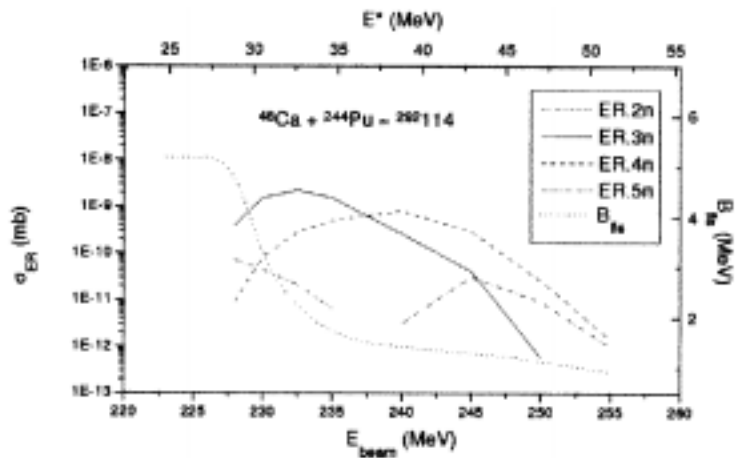


Figure 7. Excitation functions for the $^{48}\text{Ca} (^{244}\text{Pu}, xn)^{292-xn}144$ reaction.

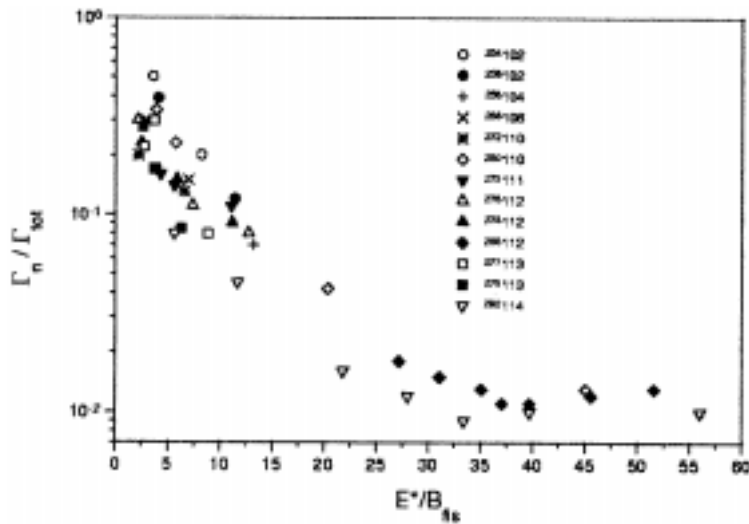


Figure 8. Systematics of the $\Gamma_n/\Gamma_{\text{tot}}$ ratio for the reaction leading to heavy nuclei with $Z = 102-114$.

This means that the ratio between the ER production and fusion cross section is mainly related (for all reactions) to the E^*/B_{fs} value, while the absolute ER value is related to the competition between the fusion and quasifission during the evolution of the dinuclear system (after capture) in the entrance channel. Therefore, the ER production (normalized to the fusion cross section) for the heavy and superheavy nuclei is mainly dependent on the E^*/B_{fs} , while the fusion process is related to the dynamic effect (the ratio between the intrinsic fusion barrier and the quasifission barrier) in the entrance channel.

References

- [1] S Hofmann, GSI-Preprint-98-16, Darmstadt, March 1998, and references therein
- [2] Yu Ts Oganessian, *Proc. of Int. Conf. Nucl. Phys. at the Turn of the Millenium* (Wilderness, South Africa, World Scientific, Singapore, 1996) p.11
- [3] A Ghiorso et al, *Nucl. Phys.* **A583**, 861 (1995); *Phys. Rev.* **C51**, R2293 (1995)
- [4] Yu A Lazarev et al, *Phys. Rev.* **C54**, 620 (1996)
- [5] G Giardina, *J. Phys.* **G23**, 1285 (1997)
- [6] Y Abe et al, *J. Phys.* **G23**, 1275 (1997)
- [7] G Giardina et al, submitted to *Nucl. Phys.*
- [8] R V Jolos et al, *JINR Preprint E4-97-302*, Dubna, 1997
- [9] G G Adamian et al, *Nucl. Phys.* **A633**, 409 (1998)
- [10] A D' Arrigo et al, *Phys. Lett.* **B34**, 1 (1994)
- [11] N V Antonenko et al, *Phys. Lett.* **B319**, 425 (1993); *Phys. Rev.* **C51**, 2635 (1995)
- [12] G G Adamian et al, *Phys. Rev.* **C56**, 373 (1997)
- [13] A J Sierk, *Phys. Rev.* **C33**, 2039 (1986)
- [14] A D' Arrigo et al, *J. Phys.* **G20**, 365 (1994)
- [15] P Möller and J R Nix, *At. Data Nucl. Data Tables* **26**, 165 (1981)
- [16] C Bhattacharya et al, *Phys. Rev.* **C53**, 1012 (1996)
- [17] M Itkis et al, to be published in *Proc. of the Int. Conf. INPC98* (Parigi, 1998)
- [18] W Q Shen et al, *Phys. Rev.* **C36**, 115 (1987)